J Mater Sci: Mater Med (2010) 21:445–450
DOI 10.1007/s10856-009-3905-z

Crystallization process of carbonate substituted hydroxyapatite nanoparticles in toothpastes upon physiological conditions: an in situ time-resolved X-ray diffraction study

A. Generosi · J. V. Rau · V. Rossi Albertini · B. Paci

Received: 28 May 2009 / Accepted: 5 October 2009 / Published online: 16 October 2009

Abstract The crystallization process in recently developed toothpastes, containing nanoparticles of carbonate substituted hydroxyapatite (nano-CHA), was investigated. For this purpose, the non-conventional Energy Dispersive X-Ray Diffraction technique, that demonstrated to be a powerful tool to follow in situ phase transformations, was applied, for the first time, to products of pharmaceutical-cosmetic interest. Two types of toothpastes, containing 15 and 20 wt% of nano-CHA, respectively, have been studied. It was observed that, after mixing the toothpastes with water and saliva in order to reproduce in vivo conditions, a crystallization of nano-CHA takes place. Such process occurs in a characteristic time of (22 ± 1) min for the toothpaste containing 15 wt% of nano-CHA and of (3.9 ± 0.5) min for the one containing 20% of nano-CHA. For both toothpastes, a 10% increase in grain dimensions was observed over an average characteristic time of (55 ± 5) min.

1 Introduction

The inorganic phase of the hard tissue of bone and teeth consists of biological apatite, similar to hydroxyapatite (HA) ($Ca_{10}(PO_4)_6(OH)_2$), but having various ionic substitutions. Enamel, containing up to 98 wt% of inorganic phase, consists of biological apatite with fewer ionic substitutions than bone and dentin mineral and more closely approximates the stoichiometric HA [1]. Hydroxyapatite is widely used in biomedicine as a coating for orthopaedic and dental implants [2–6]. It is also added to some brands of toothpastes as a polishing and whitening agent [7]. It was proved that toothpastes containing HA increase teeth brightness and whiteness, these properties being enhanced with the increase in the amount of HA [7]. Recently hydroxyapatite materials have been discovered to have remineralizing effects on the altered enamel surface, helping in the recovery of teeth microfractures and of early caries lesions [8, 9]. It is reported that the remineralization effect is increased if the particle size of hydroxyapatite is reduced down to the nanometric range. Indeed, the interaction of nanoparticles with dentine and enamel is more effective, due to the increased surface to volume ratio [10, 11].

This fact stimulated the production of new toothpastes containing nanosized hydroxyapatite and carbonate substituted hydroxyapatite [12–14], aiming to restore the damaged human enamel surface. Synthetic CHA mimics the composition, structure, morphology and nano-dimension of the enamel natural apatite. It was discovered that nanosized CHA can chemically bond to the surface of natural enamel, producing a persistent coating and filling scratches and pits, thanks to their tailored biomimetic characteristics, covering and safeguarding the enamel structure [14].

These new toothpastes stimulated the scientific discussion on possible novel applications of nanotechnologies in pharmaceutical and cosmetic products: on their safety, efficiency and action mechanisms. It should be noted, however, that the literature available, extremely scarce, reports mainly on microscopy investigations, such as Scanning Electron Microscopy and Atomic Force Microscopy.

Conversely, in the present work the non-conventional Energy Dispersive X-Ray Diffraction (EDXRD) technique was applied for the first time on the products of pharmaceutical-cosmetic interest. This technique was already

A. Generosi · J. V. Rau (✉) · V. Rossi Albertini · B. Paci
Istituto di Struttura della Materia, Consiglio Nazionale delle Ricerche, Via del Fosso del Cavaliere, 100-00133 Rome, Italy
e-mail: giulietta.rau@ism.cnr.it

successfully applied in our previous studies to follow in situ nanoparticles crystallization [15]. The EDXRD method is able to monitor in real time the structural evolution of samples in a direct and reliable way [16, 17]. Here, the crystallization of nanoparticles contained in the toothpastes was observed by means of time-resolved EDXRD. The crystallization process was monitored after mixing the toothpastes with water and saliva, in order to better simulate the physiological conditions. The advantages of using the EDXRD approach, to observe in situ phase transformations of biomaterials by collecting sequences of diffraction patterns, were discussed in detail in a previous work [15]. Here, only a brief description of the technique is reported in the experimental section, for the sake of clearness.

2 Materials and methods

2.1 Materials

The adopted experimental protocol was the following: each toothpaste as it is (containing carbonated substituted 4–8 wt% non stoichiometric hydroxyapatite) was characterized by EDXRD. The two toothpaste samples contained 15 and 20 wt% of nano-CHA, respectively. Subsequently, the structural evolution and final morphology of two new samples—15% mixture and 20% mixture, obtained by mixing the toothpastes (containing 15 and 20 wt% of nano-CHA, respectively) with water and saliva to reproduce the physiological conditions, were monitored. The 15% mixture was prepared by mixing toothpaste containing 15% of nano-CHA with water and saliva in the proportion of 2:1:1 (mass ratio) at room temperature. The 20% mixture was prepared by mixing toothpaste containing 20 wt% of nano-CHA with water and saliva in the same proportion under the same conditions. Then, each sample was positioned onto an appositely designed sample holder in the optical centre of the diffractometer for the X-ray study.

2.2 Energy dispersive X-Ray diffraction method

An X-ray diffraction pattern represents the intensity of the X-ray radiation elastically scattered by a sample, as a function of the momentum transfer Δq. The momentum transfer amplitude usually takes the name of scattering parameter and can be expressed as: $q(E, \vartheta) = a\, E \sin \vartheta$, E being the energy of the electromagnetic radiation, 2ϑ—the scattering angle and a = constant = 1.014 Å^{-1}/keV. To perform the reciprocal space scan, and namely to collect a diffraction pattern, two modes are thus available. The first, most conventional, consists of using monochromatic X-ray radiation (selecting a single energy component) and in carrying out an angular scan by the mechanical movement of the arms of the diffractometer (Angular Dispersive mode). Alternatively, a white X-ray beam can be used, fixing the scattering angle 2ϑ and executing the reciprocal space scan electronically (Energy Dispersive mode). In this case, the diffraction pattern is collected through the measurement of the energy spectrum of such polychromatic beam after it is scattered by the sample. To measure the energy spectrum, a Solid State Detector (SSD) is utilized. The latter is not only able to count the number of photons diffracted by the sample, but also to discriminate their energy. The advantage of the EDXRD on its angular dispersive counterpart is that no movement is needed during the data collection, which makes the measurement method much more reliable. Indeed, since the diffraction geometry, as well as the irradiated volume and surface, remain unchanged during the data collection, no errors coming from re-normalization to the angular-dependent irradiated zone, or from irradiation of different parts of the sample at different angles, occur. This problem is of particular concern when inhomogeneous samples are studied and/or when time resolved measurements, requiring the collections of long sequences of diffraction patterns, are carried out. Furthermore, since in the ED mode the acquisition of the diffracted signal at the various q-values is carries out simultaneously, the time is much reduced.

The measurements were executed by a non-commercial machine [16, 17], its schematic drawing is shown in Fig. 1. The polychromatic ("white") primary X-ray beam is produced by a W-anode tube (Fig. 1(*1*)) operating at 60 KV and is collimated one upstream and two downhill the sample by three W slits (Fig. 1(*2*)). The sample holder (*3*) is situated in the optical centre of the diffractometer. The detection is accomplished by an EG&G high purity germanium SSD (Fig. 1(*4*)). The detector is connected to a PC via ADCAM hardware and the signal is processed by a Maestro software, which performs the necessary analogue to digital conversions.

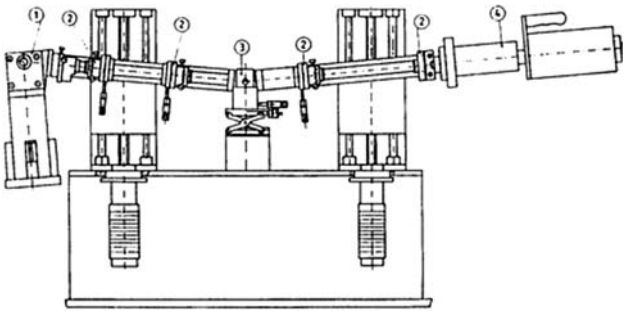

Fig. 1 Schematic drawing of the EDXRD apparatus: (*1*) X-ray W-anode tube; (*2*) Collimation slits; (*3*) Sample holder; (*4*) Solid state Ge single crystal detector

The energy resolution, in the energy region of interest (15–55 keV), is about 1.5%, while the maximum count rate is 10 kcounts/s. Source and detector arms are moved by two linear actuators driven by step motors, leading to a minimum scattering angle increment of 0.004°.

A preliminary study, aiming to individuate the q-range, containing the most intense first order crystalline reflections attributable to the nano-CHA, allowed to establish the optimal experimental conditions of the Energy Dispersive X-ray Diffraction setup. As the result of this test, the following working conditions were found: beam energy = 55 KeV, vertical aperture of the collimation slits [500–800–500] μm (in sequence from the tube to the SSD) and scattering angle $2\vartheta = 9.80°$.

3 Results and discussion

The traditional commercial toothpastes generally include water, flavouring, foaming, sweetening, viscous and brightening agents, usually well-known and characterized. Recently, new toothpastes containing bioactive particles of nano-CHA have been developed, patented [13] and marketed. Here we investigated the toothpastes containing 15 and 20 wt% of nano-CHA.

First, both (15 and 20 wt% of the nano-CHA) toothpaste samples alone were characterized by EDXRD. Subsequently, the structural evolution of two samples, obtained by mixing the toothpastes with water and saliva, were monitored by time resolved EDXRD.

Figure 2 shows the diffraction patterns collected ex situ for the two toothpastes. The peaks labelled in Fig. 2 correspond to the hydroxyapatite ($Ca_{10}(PO_4)_6(OH)_2$, hexagonal system, space group $P6_3/m$ [18]), despite the toothpastes contain carbonated substituted hydroxyapatite. This result

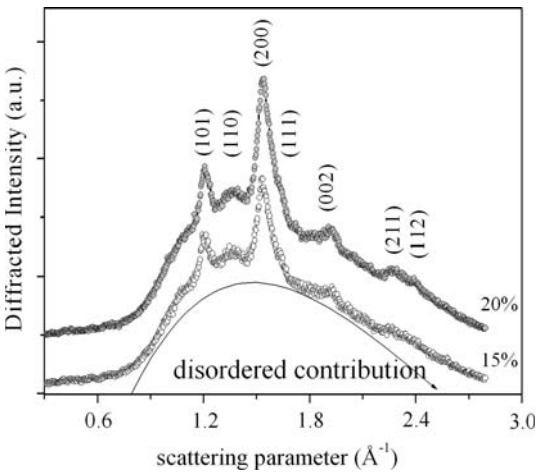

Fig. 2 Diffraction patterns of the toothpastes: lower curve—15 wt% of nano-CHA and upper curve—20 wt% of nano-CHA

was expected, since it has been previously demonstrated that up to 50 wt% of carbonate substitution of the phosphate ions in hydroxyapatite does not alter the $Ca_{10}(PO_4)_6(OH)_2$ system and space group, neither strain nor stress being detected in the crystalline cell [19]. Moreover, an amorphous component, evidenced by a black arrow and attributed to both the nano-CHA and other ingredients of the toothpaste, corresponds to the 75% of the total scattered contribution. As can be seen, the signals of both toothpaste samples well overlap, the major difference being the more intense peaks present in the diffraction pattern of the toothpaste containing 20 wt% of nano-CHA (*upper curve*).

To estimate the crystallite average size from a diffraction pattern, an equation based on the Laue relations (equivalent to the Scherrer formula valid for the Angular Dispersive X-Ray Diffraction mode only) was used [15]:

$$\frac{1}{2}t\,q_2 = (n+1)\pi \text{ and } \frac{1}{2}t\,q_1 = (n-1)\pi \qquad (1)$$

where t is the crystallites average diameter; q_1 and q_2 are the interference function zeros adjacent to the function maximum ($q_1 < q_2$); n is the order of the interference function peaks (the parameter that labels the features of the "sinc" interference function). The grain size, obtained combining these two equations, is (8 ± 2) nm. No difference is observed between the nano-CHA particles size of the two investigated toothpastes.

Then, both the toothpastes were left for 30 hours under the room conditions and during this time period, a sequence of diffraction patterns was collected. The results for the toothpaste containing 20 wt% of nano-CHA are shown in Fig. 3. As visible, the shape and position of the crystalline Bragg peaks did not change over time. Instead, a decrease of the disordered component contribution to the diffracted intensity was registered, as evidenced in the inset in Fig. 3, showing the comparison between the first (*continuous line*) and the last (*dots*) recorded spectra. This fact is attributed to the dehydration of the toothpaste, i.e. the evaporation of water present in the paste. Similar results were obtained for the toothpaste containing 15 wt% of the nano-CHA.

After this preliminary study, other two samples, labelled as 15% mixture and 20% mixture, were prepared mixing the toothpastes (15 and 20 wt% of nano-CHA, respectively) with water and saliva, in order to simulate the physiological conditions encountered in vivo.

In Fig. 4, the time evolution of the total diffracted intensity and of the nano-CHA (200) peak of the 15% mixture is presented. The diffraction patterns were collected every 60 s during the first 30 min and subsequently every 2 min, to follow in real time the structural evolution of the nano-CHA component. The quantitative total diffracted intensity loss was estimated. The amorphous contribution

strongly decreased upon time. This evolution is characterized by an induction time of approximately (9 ± 1) min, and it is well fitted by a first order exponential decay, the characteristic time being $\tau_{tot} = (18 \pm 1)$ min. Such intensity loss is accompanied by an increase in the crystalline signal intensity, as observed also for the 20% mixture. In the lower part of Fig. 4, the evolution of the (200) reflection intensity is reported. The CHA crystallization process is well fitted by a sigmoidal curve, the characteristic time being $\tau_{(200)} = (22 \pm 1)$ min, which is close to τ_{tot}, corresponding to the disordered contribution intensity loss. As can be seen, after this time interval the saturation value is reached.

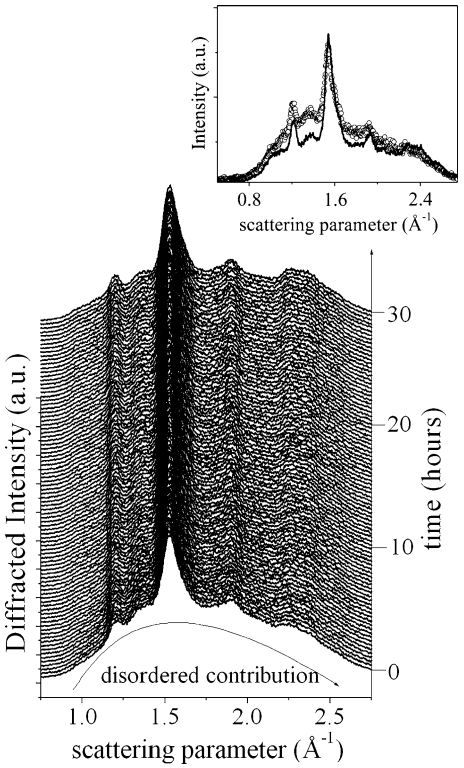

Fig. 3 Sequence of diffraction patterns collected as a function of scattering parameter q and of time, during the exposure of the toothpaste containing 20 wt% of nano-CHA to room conditions for 30 hours. In the inset, the comparison between the first (*continuous line*) and the last (*dots*) recorded spectra is plotted

In Fig. 5, the time evolution of the total diffracted intensity and of the nano-CHA (200) peak of the 20% mixture is presented. The diffraction patterns were collected every 60 s for 14 min to follow in real time the structural evolution of the nano-CHA. An effect similar to that registered for pure toothpastes was observed. Due to water evaporation, the diffracted intensity or, more precisely, the contribution of the X-ray amorphous component to the overall diffracted intensity, diminishes overtime. Along with the evaporation process, another effect contributes to the decrease of the amorphous component. It is the progressive conversion of the latter into crystalline phase. This second effect is confirmed by a corresponding increase of the Bragg reflections intensity, which partially counterbalance the decrease of the intensity diffracted by the X-ray amorphous component. The latter can be well fitted by a first order exponential decay, whose characteristic time is (2.5 ± 0.5) min.

In Fig. 5, the time evolution of the (200) reflection intensity, substantially identical to that of the other Bragg peaks, is reported. Despite the fast real time evolution, it was possible to follow the crystallization dynamics. The data of the lower curve in Fig. 5, representative of the CHA crystallization process, are well fitted by a sigmoidal curve (50% relative intensity increase), with a characteristic time of $\tau_{(200)} = (3.9 \pm 0.5)$ min, perfectly matching the disordered contribution intensity loss (−50%), which is also

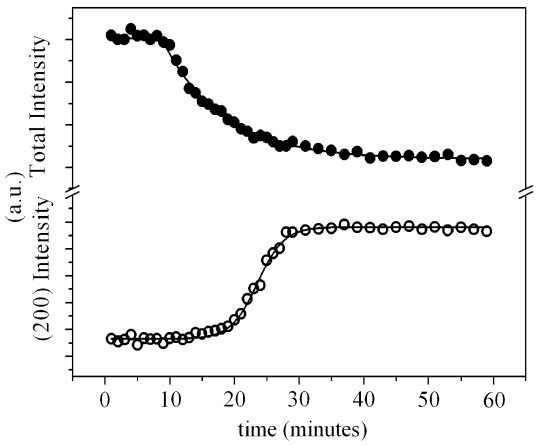

Fig. 4 Time evolution of the total diffracted intensity (*full dots*) and of the nano-CHA (200) peak intensity (*empty dots*) for the 15% mixture

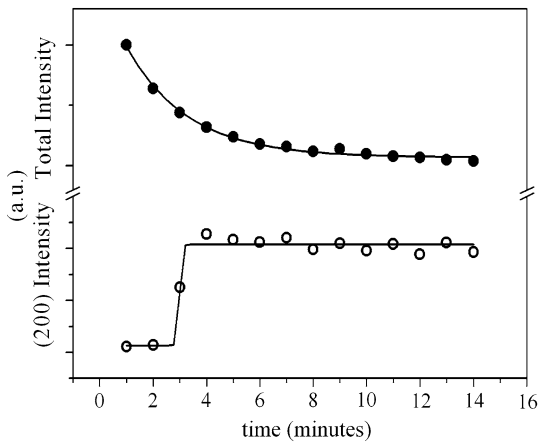

Fig. 5 Time evolution of the total diffracted intensity (*full dots*) and of the nano-CHA (200) peak intensity (*empty dots*) for the 20% mixture

reported (*higher curve* in Fig. 5). As can be seen in Fig. 5, after this time interval, the process saturates.

The obtained results demonstrate that the interaction between toothpaste, water and saliva leads to the nano-CHA crystallization. Under physiological conditions, both toothpastes (the 20% mixture and the 15% mixture) have similar behaviour. The only difference lays in the crystallization process rates, which are obviously influenced by the different nano-CHA content. A higher concentration of nanoparticles is expected to favorite their aggregation (to which the formation of larger crystals is due). Indeed, a higher nano-CHA content provides a larger amount of nucleation centers and of available coalescing material, so that, in order to reach a certain degree of crystallinity, a shorter time is required.

Likely, both components—water and saliva—are important for the crystallization process. Literature data report greater solubility of calcium and phosphate ions in saliva leading to the fast growth of highly crystalline hydroxyapatite particles [20].

Moreover, by an accurate analysis of the sequences of the EDXRD patterns it was possible to deduce the evolution of the nano-CHA particle's size for the 20% mixture and the 15% mixture. The Scherrer equations were used for this purpose, as previously described in ref. [15]. In Fig. 6, the (200) crystallite average dimension is plotted as a function of time. As visible, in both toothpastes (independently on the nano-CHA content) the grain size evolution over time follows a sigmoidal growth, with the total increase of about 10% and with characteristic times coinciding within the experimental error bar ($\tau_{20\%\ \text{mixture}} = (50 \pm 5)$ min and $\tau_{15\%\ \text{mixture}} = (59 \pm 5)$ min).

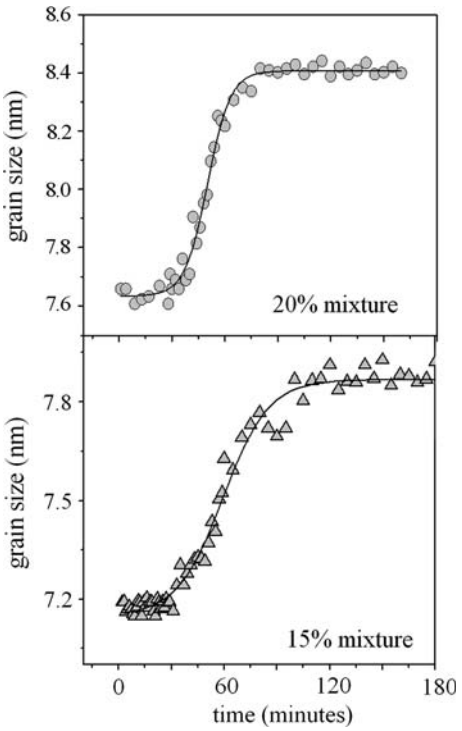

Fig. 6 Time evolution of the (200) crystallites dimension for the 15% mixture (*lower curve*) and for the 20% mixture (*upper curve*)

Based on the results of this work one can conclude that the structural characteristics of the nano-CHA embedded in the toothpaste amorphous matrix are fully consistent with the ones, previously published by us in Ref. [15], of the pure nano-HA.

4 Conclusions

The application of the non-conventional EDXRD technique, to follow in situ phase transformations of pharmaceutical-cosmetic products, is reported. The structural evolution of the nano-sized carbonate substituted hydroxyapatite contained in newly developed toothpastes, mixed with water and saliva, was monitored. It was found that the crystallization rate depends on the nano-CHA content. The conversion of the disordered nano-CHA into crystalline domains occurs with the following characteristic times: (22 ± 1) min for the toothpaste containing 15 wt% of nano-CHA and (3.9 ± 0.5) min for the toothpaste containing 20 wt% of CHA.

Moreover, the time evolution of the nano-CHA particle's grain size was estimated. For both toothpastes a 10% increase in crystalline grain dimensions, upon an average characteristic time of (55 ± 5) min, was observed, proving the nucleation process to be independent on the nano-CHA content.

References

1. Dorozhkin SV. Calcium orthophosphates in nature, biology and medicine. Materials. 2009;2:399–498.
2. Suchanek W, Yoshimura M. Processing and properties of hydroxyapatite-based biomaterials for use as hard tissue replacement implants. J Mater Res. 1998;13:94–117.
3. Willmann G. Coating of implants with hydroxyapatite—material connections between bone and metal. Adv Eng Mater. 1999;1:95–105.
4. Sun L, Berndt CC, Cross KA, Kucuk A. Material fundamentals and clinical performance of plasma-sprayed hydroxyapatite coatings. J Biomed Mater Res B Appl Biomater. 2001;58:570–92.
5. Ong JL, Chan DCN. Hydroxyapatite and their use as coatings in dental implants: a review. Crit Rev Biomater Eng. 1999;28:667–707.
6. Hench LL. Bioceramics. J Am Ceram Soc. 1998;81:1705–28.
7. Niwa M, Sato T, Li W, Aoki H, Aoki H, Daisaku T. Polishing and whitening properties of toothpasete containing hydroxyapatite. J Mater Sci Mater Med. 2001;12:277–81.
8. Yamagishi K, Onuma K, Suzuki T, Okada F, Tagami J, Otsuki M, et al. A synthetic enamel for rapid tooth repair. Nature. 2005;433:819.

9. Onuma K, Yamagishi K, Oyane A. Nucleation and growth of hydroxyapatite nanocrystals for nondestructive repair of early caries lesions. J Cryst Growth. 2005;282:199–207.
10. Lv K, Zhang J, Meng X, Li X. Remineralization effect of the nano-HA toothpaste on artificial caries. Key Eng Mater. 2007;330–332(Pt.1,Bioceramics):263–6.
11. Webster TJ, Ergun C, Doremus RH, Siegel RW, Bizios R. Specific proteins mediate enhanced osteoblast adhesion on nanophase ceramics. J Biomed Mater Res. 2000;51:475–83.
12. Meng Y, Li C. Study on application of nano hydroxyapatite in toothpaste. Riyong Huaxue Gongye (Chin). 2006;36(2):131–3.
13. Guaber SPA, Gazzaniga G, Roveri N, Rimondini L, Palazzo B, Iafisco M, Gualandi P. EU Patent PCT/EP2006/005146; 2006.
14. Roveri N, Battistella E, Foltran I, Foresti E, Iafisco M, Lelli M, et al. Synthetic biomimeticcarbonate-hydroxyapatite microparticles for enamel remineralization. Adv Mater Res. 2008;47–50:821–4.
15. Rau JV, Generosi A, Ferro D, Minozzi F, Paci B, Rossi Albertini V, et al. Mater Sci Eng. 2009;C29:1140–3.
16. Felici R, Cilloco F, Caminiti R, Sadun C, Rossi V. Italian Patent No. RM 93 A 000410l; 1993.
17. Caminiti R, Rossi Albertini V. Review on the kinetics of phase transitions observed byenergy dispersive X-ray diffraction. Int Rev Phys Chem. 1999;18:263–99.
18. International Centre for Diffraction Data. Database JCPDS; 2000.
19. Legeros RZ, Trautz OR, Legeros JP, Klein E, Shirra WP. Apatite crystallites: effect of carbonate on morphology. Science. 1967;155:1409.
20. Park SW, Lee YK, Kim YU, Kim MC, Kim KN, Choi BJ, et al. Engineer. Mater. 2005;35:284–6.